

Coherence resonance in a Hodgkin-Huxley neuron

Sang-Gui Lee,¹ Alexander Neiman,² and Seunghwan Kim¹

¹*Nonlinear and Complex Systems Laboratory, Department of Physics and Mathematics, Pohang University of Science & Technology, San 31 Hyojadong, Pohang, 790-784 Korea*

²*Department of Physics, Saratov State University, Saratov 410073, Russia*

(Received 29 July 1997; revised manuscript received 7 October 1997)

We study the nonlinear response of the Hodgkin-Huxley model without external periodic signal to the noisy synaptic current near the saddle-node bifurcation of limit cycles. The coherence of the system, estimated from the interspike interval histogram and from the power spectra of membrane potentials and spike trains, is maximal at a certain noise intensity, so that the coherence resonance occurs. The mechanism of this phenomenon is found to be different from previously studied models of coherence resonance and explained in terms of rigid excitations of periodic oscillations, and the combined effect of amplitude and phase fluctuations. [S1063-651X(98)00903-9]

PACS number(s): 87.22.Jb, 05.40.+j

One of the major motivations of stochastic resonance (SR) studies [1–3] is its application in biology, and in particular in excitable neuronal systems. It has been shown both experimentally [4] and theoretically [5] that the ability of sensory neurons to process weak input signals can be enhanced by adding noise to the system. Moreover, as it has been shown recently, nonlinear systems with noise can display SR-like behavior even without external signal [6–9]. This phenomenon has been called *autonomous SR* [6] or *coherence resonance* (CR) [7]. Originally CR has been found in a simple dynamical system in the vicinity of a saddle-node bifurcation [6]. Due to nonuniformity of the noise-induced limit cycle [10], the signal-to-noise ratio, defined as the product of the height of the noise-induced peak in the power spectrum and the quality factor of this peak, displays a bell-shaped maximum as a function of the noise level. In [9] a general mechanism of CR has been proposed for nonlinear dynamical systems at the onset of saddle-node bifurcations. The CR also has been studied in excitable systems [7,8]. In [7], CR is studied for the Fitz Hugh–Nagumo model near supercritical Hopf bifurcation, using the correlation time and statistics of the activation and the excursion times as measures of coherence. The CR in bursting neuron models with subthreshold oscillations (Plant and Hindmarsh-Rose models) has also been studied, using interspike interval histograms and spike train power spectra [8].

In this paper we study CR in a Hodgkin-Huxley neuron model, which serves as a paradigm for modeling of spiking neurons [11]. We will show that the mechanism of CR in this system is different from that in the Fitz Hugh–Nagumo model since the Hodgkin-Huxley model is associated with a saddle-node bifurcation of *limit cycles*. In our case, the excitation is *rigid*, that is, there is a strong tendency that not a single oscillation but a train of several periodic oscillations are induced by noise. This is due to the tangential nature of the saddle-node bifurcation, where the subthreshold dynamics tend to spend more time in the laminar stretch near the “ghost” limit cycle with noise providing a mechanism for slow escape and reinjection. Another distinct feature of the Hodgkin-Huxley model with additive forcing is that, for a weak noise trains of several periodic oscillations appear in-

termittently, which produces phase fluctuation; for a strong noise large fluctuations in both the amplitude and the phase of the periodic motion are found. The CR phenomenon for a Hodgkin-Huxley neuron under synaptic noisy current is studied by analyzing both the time series of the membrane potential and the classical measures of neuroscience, that is, the spike train and the interspike interval histogram (ISIH). Our study should help to obtain a more comprehensive understanding of CR in excitable systems together with the studies of CR in systems with a Hopf bifurcation [7] and a saddle-node bifurcation on a circle [6].

The Hodgkin-Huxley model describes the spiking behavior and refractory properties of real neurons and serves as a paradigm for spiking neurons based on nonlinear conductance of ion channels [11]. The model is given by four nonlinear coupled equations, one for the membrane potential V , and three for gating variables, m , n , and h :

$$\begin{aligned} \frac{dV}{dt} &= I_{\text{ion}} + I_{\text{ext}} + I_{\text{syn}}, \\ \frac{dm}{dt} &= \frac{m_{\infty}(V) - m}{\tau_m(V)}, \\ \frac{dh}{dt} &= \frac{h_{\infty}(V) - h}{\tau_h(V)}, \\ \frac{dn}{dt} &= \frac{n_{\infty}(V) - n}{\tau_n(V)}, \end{aligned} \quad (1)$$

where

$$I_{\text{ion}} = -g_{\text{Na}}m^3h(V - V_{\text{Na}}) - g_{\text{K}}n^4(V - V_{\text{K}}) - g_{\text{l}}(V - V_{\text{l}}). \quad (2)$$

Dynamics of the membrane potential is driven by three types of currents: ionic current I_{ion} , external stimulus current I_{ext} , and synaptic current I_{syn} . The ionic current I_{ion} is related to the gating variables of m , n , h and describes the ionic transport through the membrane. The constants g_{Na} , g_{K} , and g_{l} are the maximal conductances for ion and leakage channels,

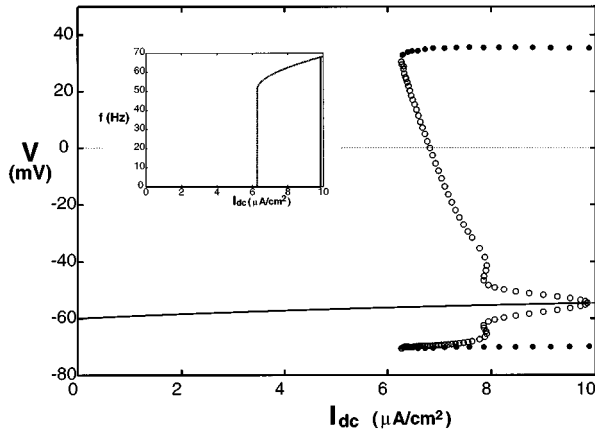


FIG. 1. Bifurcation diagram of a Hodgkin-Huxley neuron under dc current. Here I_{dc} is the bifurcation parameter and V is the membrane potential of the limit states. A solid line represents the stable fixed point, filled and unfilled circles represent membrane potentials of stable and unstable limit cycles, respectively. Inset: The frequency f of the stable limit cycle for the Hodgkin-Huxley neuron as a function of I_{dc} . The dotted line is for increasing I_{dc} and the solid line for decreasing I_{dc} .

and V_{Na} , V_K , V_l are the corresponding reversal potentials; m_∞ , h_∞ , n_∞ and τ_m , τ_h , τ_n represent the saturation values and the relaxation times of the gating variables. Detailed values of parameters can be found in [11–13]. In this study we take the external stimulus to be time independent dc current $I_{ext}(t) = I_{dc}$ which serves as a bifurcation parameter of the system.

The synaptic current represents the sum of the current inputs from all synapses connected to the other neurons. This synaptic current is found to be noisy [14], which we model as an additive noise from an Ornstein-Uhlenbeck process:

$$\tau_d \frac{dI_{syn}}{dt} = -I_{syn} + \sqrt{2D}\xi(t), \quad (3)$$

where $\xi(t)$ is Gaussian white noise, and D and τ_d are the intensity and the correlation time of the synaptic noise, respectively. In numerical simulations we take $\tau_d = 2$ msec. Numerical integration of Eq. (1) has been done using the fourth order Runge-Kutta method and the exponentially correlated synaptic noise in Eq. (3) using the method of Fox *et al.* [15] with the integration time step $\Delta t = 0.02$ msec.

Let us consider first the bifurcations in the system (1) in the absence of noise ($D = 0$). The bifurcation diagram for the membrane potential V as a function of I_{dc} is shown in Fig. 1 [16–19]. The birth of limit cycles occurs at $I_{dc} = I_c \approx 6.2 \mu A/cm^2$ due to the saddle-node bifurcation of periodic orbits. The unstable part of the periodic orbits dies at $I_{dc} = I_h \approx 9.8 \mu A/cm^2$ through the inverse Hopf bifurcation. Thus in the parameter region $I_{dc} < I_c$ the fixed point is the global attractor of the system, while for $I_c < I_{dc} < I_h$ the system possesses two coexisting stable attractors, the fixed point and the limit cycle. The dependence of the firing rate as a function of I_{dc} is shown in the inset of Fig. 1.

The focus of interest is the parameter region near the onset of the saddle-node bifurcation of periodic orbits. In our numerical experiments, we use three subthreshold values of dc currents of $I_{dc} = 5.0, 5.5,$ and $6.0 \mu A/cm^2$. With noise taken into account, the system either fluctuates around the fixed point or makes an excursion into the region of the limit cycle, inducing the trains of periodic oscillations of the membrane potentials. The time series of the membrane potential V for four different values of noise intensity for $I_{dc} = 6.0 \mu A/cm^2$ are shown in Fig. 2. For small noise intensity [Fig. 2(a)] the system spends most of its time fluctuating around the rest potential $V_{rest} = -65$ mV, and displays trains of a few short periodic oscillations, characteristic of the so-called “rigid excitation.” This rigid excitation appears when the system in the subthreshold regime spends more time in the narrow corridorlike neighborhood of the remnants of the limit cycles due to the tangential nature of the saddle-node bifurcation of limit cycles [20]. The noise-controlled time

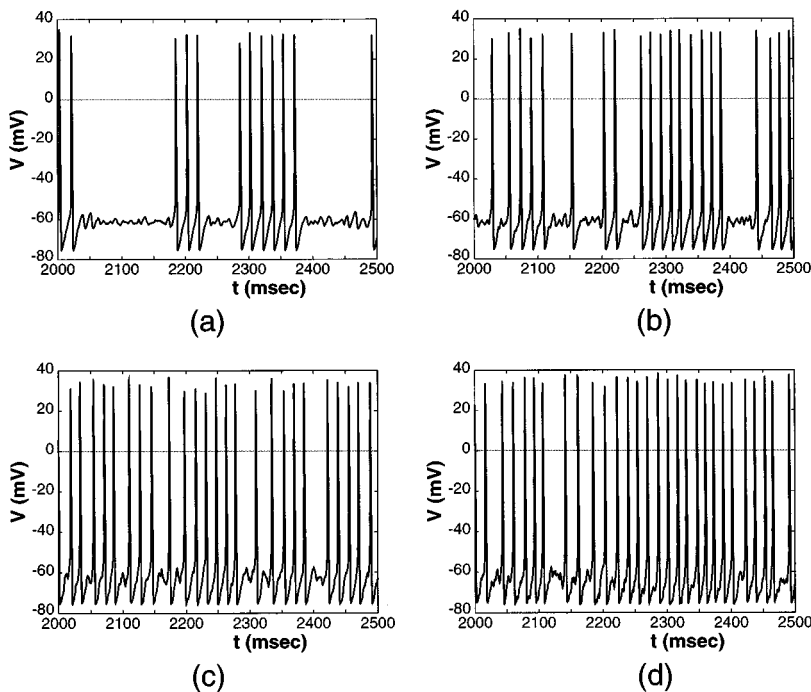


FIG. 2. Time series of the membrane potential V for $I_{dc} = 6 \mu A/cm^2$ for various noise intensity: (a) $D = 1$, (b) $D = 5$, (c) $D = 10$, and (d) $D = 20$.

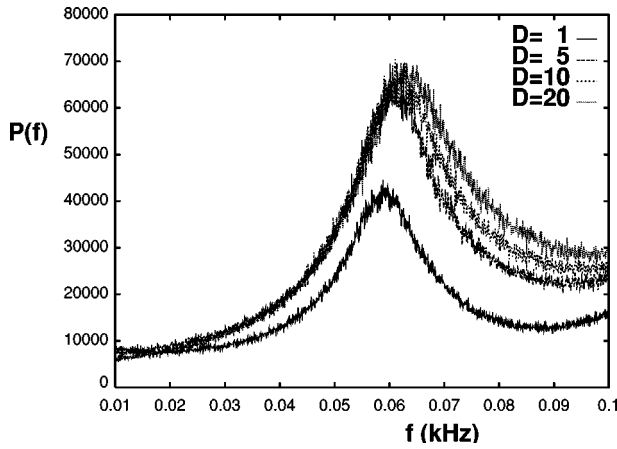


FIG. 3. Power spectra of the membrane potentials in Fig. 2: $D = 1, 5, 10,$ and 20 from the bottom curve to the top, respectively. The coherent SNR is calculated from the peak of each power spectra.

scale of the system is the mean time to drive the system to the limit cycle region, or activation time T_a . For a weak noise this time scale is closely akin to the Kramers time of bistable systems and therefore depends on D according to the exponential Arrhenius law [21] as $T_a \propto \exp(\text{const}/D)$. Another time scale is the period of oscillations of the limit cycle, T_0 . This time scale has mainly a deterministic origin from the bifurcation structure and depends on noise only slightly (see the inset of Fig. 1). For a weak noise, $T_a \gg T_0$, so that in the time series of the membrane potential the two branches, the fluctuations around the fixed point and rare periodic oscillation trains, are well separated from each other. The system has a pure stochastic nature in this case. With the increase of noise intensity the activation time decreases rapidly and the mean length of periodic trains increases. Thus the motion of the system becomes more coherent [see, e.g., Fig. 2(b)].

With further increase of noise, activation time becomes very short, $T_a < T_0$, so that the two regimes of the system cannot be separated well [Figs. 2(c), 2(d)]. In this case periodic oscillations become affected by noise itself. Thus the noise affects the dynamics of the system in two ways. On one hand, with the increase of noise the system spends more time in the oscillating regime which makes the membrane potential more coherent. However, on the other hand, noise also affects the periodic oscillations, leading to the well-known effect of amplitude and phase fluctuations. This tendency indeed leads to stochastization of the membrane potential. The competition of these two tendencies should result to an optimal noise level at which the coherence of the motion of the system is maximal, i.e., manifestation of the coherence resonance.

First, we characterize the effect quantitatively through the power spectra $P(f)$ from the membrane potential. The power spectra $P(f)$ computed from 200 averages of the power spectra for the time series of the membrane potential with length 131 072 using a fast Fourier transform are shown in Fig. 3 for various values of noise intensity. For a weak noise ($D=1$ in Fig. 3) the height of the noise-induced peak in the power spectrum is very small. With the increase of noise ($D=5$) the height increases and the peak becomes very well

pronounced. However, with further increase of noise ($D=10, 20$) the height of the peak starts to saturate and the width of the peak increases faster than its height, so that the peak becomes difficult to resolve from the noise background again. Note that the position of the peak shifts to the right as the noise intensity increases. This is due to the increase in firing rate of the Hodgkin-Huxley neuron as I_{dc} increases (see the inset of Fig. 1). To characterize the behavior of the peak quantitatively, we compute a measure of coherence β_s , defined in Ref. [6] as the product of the height of the peak H to its quality factor Q_s as

$$\beta_s = H Q_s, \quad Q_s = \frac{\omega_p}{\Delta\omega}, \quad (4)$$

where ω_p is the frequency at which the peak occurs and $\Delta\omega$ is the width of the peak at the half maximum height. The peak is fitted using splines and the width of the fitted curve is computed to estimate $\Delta\omega$. This quantity β_s can be associated with the signal-to-noise ratio and its dependence on the noise intensity is shown in Fig. 4(a). The well-expressed maximum of the curve $\beta_s(D)$ indicates that CR occurs at an optimal noise intensity, for example, $D \approx 3$ when $I_{dc} = 6.0 \mu\text{A}/\text{cm}^2$. Note that as I_{dc} increases the system moves closer to the bifurcation point, leading to a reduction in the size of the optimal noise intensity.

The occurrence of CR can be more clearly understood from the analysis of the functional dependence of H and $\Delta\omega$ on the noise. The curves of H and $\Delta\omega$ as a function of noise intensity are fitted to be $H \sim a \exp(-b/D)$ and $\Delta\omega \sim c + dD$ with appropriate constants a , b , c , and d [Fig. 4(b)]. The exponential dependence of H on D describes the mean escape rate from the rest state without action potentials to the oscillatory state with periodic action potentials [Fig. 2(a)]. The linear dependence of $\Delta\omega$ on D is due to the fluctuation of frequencies of noise-induced oscillations. For a weak noise, coherent signal-to-noise ratio (SNR) increases due to the sharp increase in H because in this case $\Delta\omega \sim c$ and $H \sim a \exp(-b/D)$. But for a large noise, coherent SNR decreases due to the increase in $\Delta\omega$ because $\Delta\omega \sim dD$ and $H \sim a$ in this regime. The CR in the Hodgkin-Huxley neuron model is a consequence of these combinations of asymptotic behaviors.

The mechanism, described above, differs from CR in the Fitz Hugh–Nagumo model where the Hopf bifurcation takes place [7]. In the Hodgkin-Huxley system noise induces transitions from the fixed point to a train of several periodic oscillations, or rigid excitation, while in the case of the Hopf bifurcation noise kicks the system out of the fixed point leading to a single isolated oscillation only. This difference leads to different behaviors in statistical measures of the systems, β_s . For comparison, we computed a measure of coherence in the Fitz Hugh–Nagumo model with the same parameters as in [7]. The width $\Delta\omega$ (or Q) of the noise-induced peak shows a minimum (or maximum) near the optimal noise intensity with maximal CR [22] but in the Hodgkin-Huxley model, the width $\Delta\omega$ does not show a minimum as seen in Fig. 4(b). The main difference between the functional shapes for weak noise is due to the rigid excitations in the Hodgkin-Huxley neuron model and isolated oscillations in the Fitz Hugh–Nagumo model for weak noise. The periodicity of

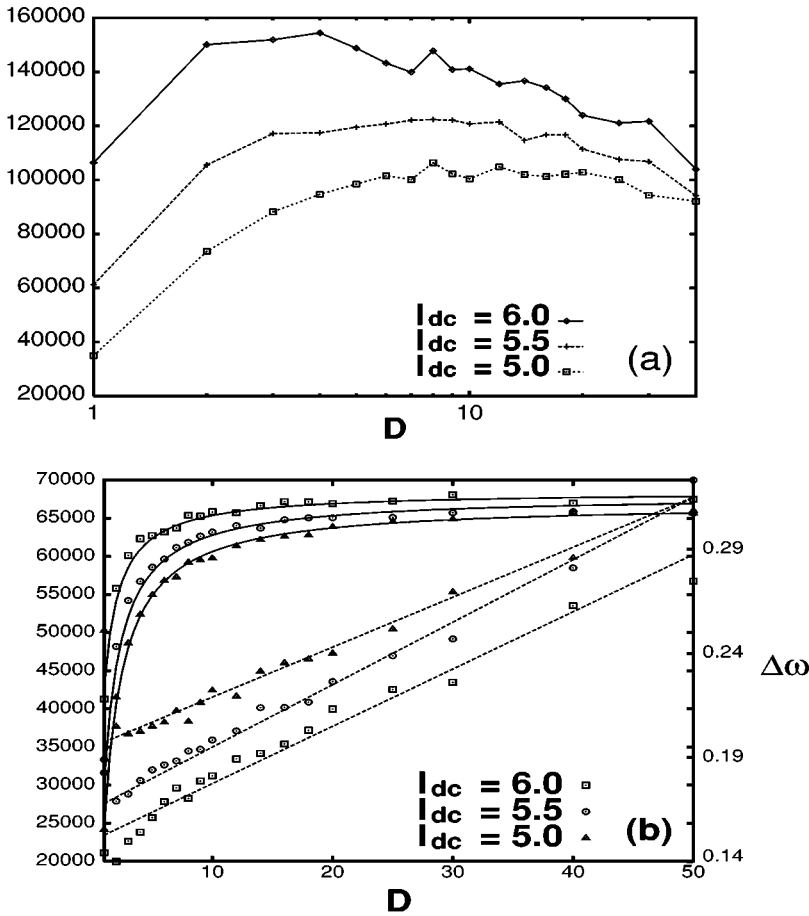


FIG. 4. (a) The measure of coherence, β_s , computed from the power spectrum, versus noise intensity D and (b) the dependence of H and $\Delta\omega$ on D . Rectangles are for $I_{dc} = 6.0 \mu A/cm^2$, circles $I_{dc} = 5.5 \mu A/cm^2$, and triangles $I_{dc} = 5.0 \mu A/cm^2$. The solid line is for a fitting curve H with $a \exp(-b/D)$ and the dashed lines for $\Delta\omega$ with $c + dD$, with constants a , b , c , and d .

oscillations in the case of rigid excitations is quite uniform so that $\Delta\omega$ defined from the power spectrum remains small for weak noise. But in the Fitz Hugh–Nagumo model the intervals between isolated oscillations show strong fluctuations for weak noise to yield a large value of $\Delta\omega$.

The spike train provides an efficient way to code a sequence of action potentials with nearly the same shape since the most important information in neuronal systems is widely believed to be coded in the time sequence of action potential generations [23]. The spike train is a binary time series with a value 1 at the time of action potential generations and 0 at other times. We analyzed coherent SNR for spike trains by representing the time series of the membrane potential with length 131 072 as a sum of δ functions:

$$V(t) = \sum_{i=1}^N \delta(t - t_i), \quad (5)$$

where t_i are the time at which the i th spike occurs and N is the number of spikes in the time series. The power spectral analysis of the coherent SNR of spike trains by fast Fourier transform is shown in Fig. 5, which exhibits CR at nearly the same value of noise intensity as one from the membrane potential in Fig. 4(a). This is because the time interval between any two subsequent spikes is quite uniform due to the rigidity of periodic action potential generations, which enhances the peak structure in the power spectrum and coher-

ent SNR. It is quite interesting to find that CR is also well coded in spike trains in the case of the Hodgkin-Huxley neurons.

The results of calculation of the ISIH for $I_{dc} = 6.0 \mu A/cm^2$ are shown for various noise intensities in Fig. 6. A typical ISIH possesses a maximum close to the mean period of oscillations (reciprocal of the mean firing rate). For a weak noise the activation time is very large and the contribution of periodic motion to the whole spike train is small. As a result the distribution of activation times possesses a long tail and a small maximum around the mean period of

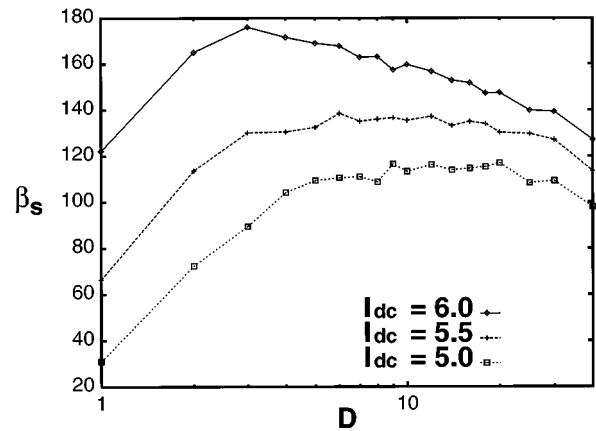


FIG. 5. Coherent SNR, β_s , versus noise intensity, D , from spike trains for $I_{dc} = 5.0, 5.5$, and $6.0 \mu A/cm^2$.

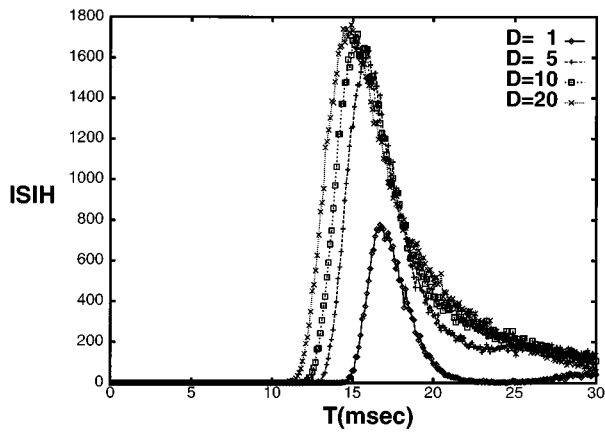


FIG. 6. Interspike interval histograms at $I_{dc} = 6.0 \mu\text{A}/\text{cm}^2$ for various values of noise intensity, $D = 1, 5, 10,$ and 20 .

oscillations. With the increase of noise the height of the peak increases. This is indeed the result of the decrease of the activation time and the enhancement of the oscillation trains of the membrane potential. For large enough noise the growth of the height saturates and the width of the peak increases, as noise leads to an increase in fluctuations around the mean firing rate. The crucial point here is that the height and the width of the peak depend on noise intensity differently [9]. A measure of coherence for the ISIH can be constructed in analogy with that for the power spectrum of the membrane potential time series in Eq. (4),

$$\beta_i = H Q_i, \quad Q_i = \frac{T_p}{\Delta T}, \quad (6)$$

where H is the height of the peak in the ISIH plot, T_p is the interspike interval of the peak, and ΔT is the width of the peak at the half height. The coherence measure β_i is shown in Fig. 7, which displays a well-pronounced maximum. It is found that this coherence resonance occurs at about the same value of D as one for the coherence measure computed from the power spectrum in Fig. 4.

Beyond the bifurcation point $I_c < I_{dc} < I_h$ the system exhibits a kind of stochastic bistability between two metastable states, the fixed point and the stable limit cycle separated by an unstable limit cycle. In this case CR can be observed also with the mechanism very similar to the previous case. For a weak noise the system spends a long time in the basin of attraction of the fixed point and rarely makes a transition to

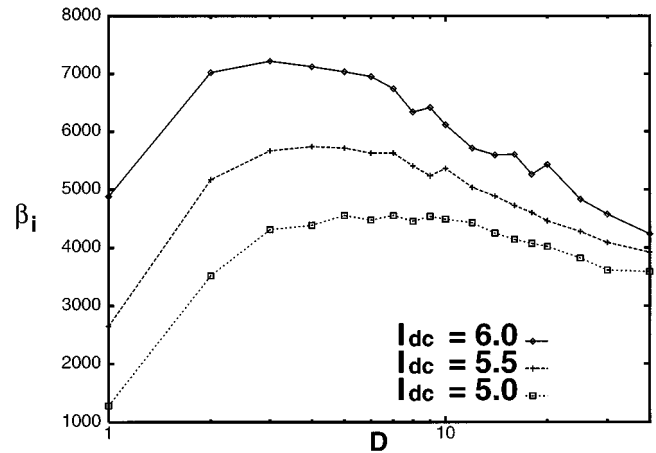


FIG. 7. The coherence measure, β_i , computed from the interspike interval histogram, versus D for $I_{dc} = 5.0, 5.5,$ and $6.0 \mu\text{A}/\text{cm}^2$.

the limit cycle. For an optimal noise intensity, when the activation time is small and is of order of the period of oscillations, the dynamics of the system is most coherent. However, larger noise influences dramatically the periodic oscillations leading to the amplitude and phase fluctuation and therefore destroys the coherence.

In conclusion, we have studied the coherence resonance in the Hodgkin-Huxley neuron model. This model, which is a paradigm for studies of spiking neurons, possesses a saddle-node bifurcation of limit cycles which makes it different from other models whose CR has been already studied. The synaptic noise current affects the dynamic of the system in two ways.

(i) The increase of noise intensity decreases the activation time so that the contribution of the periodic motion increases. This tendency enhances the coherence of the membrane potential.

(ii) Noise also results in the amplitude and phase fluctuations of the periodic motion destroying periodicity in the system. The competition of these two mechanisms gives the coherence resonance: the coherence of the system (quantified both from the power spectra of membrane potentials and spike trains and from the interspike interval histogram) is maximal for an optimal noise level.

The work was supported in part by the Ministry of Education (Grant No. BSRI-96-2438). We would like to thank H. Kook and S. K. Han for helpful discussions.

[1] R. Benzi, A. Sutera, and A. Vulpiani, *J. Phys. A* **14**, L453 (1981); R. Benzi, G. Parisi, A. Sutera, and A. Vulpiani, *Tellus* **34**, 10 (1982); C. Nicolis, *ibid.* **34**, 1 (1982).
 [2] Proceedings of the NATO Advanced Research Workshop on Stochastic Resonance in Physics and Biology, edited by F. Moss, A. Bulsara, and M. F. Shlesinger [*J. Stat. Phys.* **70** (1993)]; Proceedings of the International Workshop on Fluctuations in Physics and Biology: Stochastic Resonance, Signal Processing and Related Phenomena, edited by R. Mannella and P. V. E. McClintock [*Nuovo Cimento D* **17** (1995)].

[3] F. Moss, in *Some Contemporary Problems in Statistical Physics*, edited by G. Weiss (SIAM, Philadelphia, 1994); F. Moss, D. Pierson, and D. O'Gorman, *Int. J. Bifurcation Chaos* **4**, 1383 (1994); K. Wiesenfeld and F. Moss, *Nature (London)* **373**, 33 (1995); A. R. Bulsara and L. Gammaitoni, *Phys. Today* **49** (3), 39 (1996); a full bibliography can be found at World Wide Web site <http://www.pg.infn.it/sr/>.
 [4] H. A. Braun, H. Wissing, K. Schäfer, and M. C. Hirsh, *Nature (London)* **367**, 270 (1994); J. K. Douglass, L. Wilkens, F. Pantzelou, and F. Moss, *ibid.* **365**, 337 (1993).

- [5] K. Wiesenfeld, D. Pierson, E. Pantazelou, C. Dames, and F. Moss, *Phys. Rev. Lett.* **72**, 2125 (1994); A. Longtin, *J. Stat. Phys.* **70**, 309 (1993); F. Moss, *Ber. Bunsenges. Phys. Chem.* **95**, 303 (1991).
- [6] Hu Gang, T. Ditzinger, C. Z. Ning, and H. Haken, *Phys. Rev. Lett.* **71**, 807 (1993).
- [7] A. S. Pikovsky and J. Kurths, *Phys. Rev. Lett.* **78**, 775 (1997).
- [8] A. Longtin, *Phys. Rev. E* **55**, 868 (1997).
- [9] A. Neiman, P. Saparin, and L. Stone, *Phys. Rev. E* **56**, (to be published).
- [10] W.-J. Rappel and S. H. Strogatz, *Phys. Rev. E* **50**, 3249 (1994).
- [11] A. L. Hodgkin and A. F. Huxley, *J. Physiol. (London)* **117**, 500 (1952).
- [12] S. Kim, H. Kook, J. H. Shin, and S. G. Lee (unpublished).
- [13] D. Hansel, G. Mato, and C. Meunier, *Phys. Rev. E* **48**, 3470 (1993).
- [14] A. Arieli, D. Shoham, R. Hildesheim, and A. Grinvald, *J. Neurophysiol.* **73**, 2072 (1995).
- [15] R. F. Fox, I. R. Gatland, R. Roy, and G. Vemuri, *Phys. Rev. A* **38**, 5938 (1988).
- [16] B. Hassard, *J. Theor. Biol.* **71**, 401 (1978).
- [17] J. Rinzel, *Federation Proc.* **37**, 2793 (1978).
- [18] W. C. Troy, *Q. Appl. Math.* **36**, 73 (1978).
- [19] J. Rinzel and R. N. Miller, *Math. Biosci.* **49**, 27 (1980).
- [20] S. H. Strogatz, *Nonlinear Dynamics and Chaos* (Addison Wesley, New York, 1994).
- [21] P. Hänggi, P. Talkner, and M. Borkovec, *Rev. Mod. Phys.* **62**, 251 (1990).
- [22] S. G. Lee and S. Kim (unpublished).
- [23] G. P. Moore, D. H. Perkel, and J. P. Segundo, *Annu. Rev. Physiol.* **28**, 493 (1966).